Journal of Power Sources 189 (2009) 191–196

Contents lists available at ScienceDirect

Journal of Power Sources

journal homepage: www.elsevier.com/locate/jpowsour

Characterization of all-solid-state secondary batteries with $LiCoO_2$ thin films prepared by ECR sputtering as positive electrodes

Masaya Takahashi*, Masahiko Hayashi, Takahisa Shodai

NTT Energy and Environment Systems Laboratories, Nippon Telegraph and Telephone Corporation, 3-1 Morinosato Wakamiya, Atsugi, Kanagawa 243-0198, Japan

ARTICLE INFO

Article history:
Received 20 June 2008
Received in revised form
24 September 2008
Accepted 26 September 2008
Available online 10 October 2008

Keywords:
All-solid-state lithium secondary battery
Electron cyclotron resonance plasma sputtering
$LiCoO_2$ film
Charge–discharge cycle performance
Crystallinity of the $LiCoO_2$ film

ABSTRACT

We fabricated all-solid-state lithium secondary batteries consisting of $LiCoO_2$ thin films prepared by electron cyclotron resonance (ECR) sputtering LiPON and metallic lithium films, and investigated the influence of the sputtering target composition on the performance of the batteries and $LiCoO_2$ films. We found that the $LiCoO_2$ film sputtered with a stoichiometric $LiCoO_2$ target included many impurities (mainly Co_3O_4) and these impurities were eliminated by adding an excess of Li source to the sputtering target to achieve a Li/Co atomic ratio of 2.0 elsewhere. The $LiCoO_2$ film sputtered with a Li2.0 target exhibited a larger discharge capacity and a high performance level for large current operation. However, the capacity of a battery employing $LiCoO_2$ film sputtered with a Li2.0 target decreased more rapidly than that with a Li1.0 or Li1.7 target in a charge–discharge cycle test. We also investigated the cycle performance of $LiCoO_2$ films in an ordinary liquid electrolyte by using beaker type cells. We found that the decrease in capacity during the cycle tests was caused by the deterioration of the $LiCoO_2$ film, because the dependence of the target composition on the cycle performance in the beaker type cells was similar to that in the all-solid-state cells. We consider the capacity decrease to be caused by the deterioration in the crystallinity of the $LiCoO_2$ film when using the Li2.0 target and caused by the formation of a Co_3O_4 layer on the surface of the $LiCoO_2$ film when using a Li1.7 target on basis of the results of X-ray diffraction analysis and Raman spectroscopy.

1. Introduction

Recently, the size and weight of portable electronic devices, including mobile phones, laptop computers and portable music players, has been decreasing rapidly. However, if we are to produce smaller and lighter devices, we must develop small high power batteries. A promising candidate is a thin-film lithium secondary battery consisting of a positive electrode film, a solid electrolyte and a negative electrode film formed on a substrate. This battery has various advantages including no liquid leakage, excellent safety, a long cycle life and a wide operating temperature range [1–8]. Moreover, it is possible to make a flexible battery if we fabricate the thin-film battery on a flexible polymer film. Battery flexibility in bend enhances the flexibility with which we can arrange batteries in devices.

Many lithiated transition metal oxides have been investigated intensively as cathode materials for lithium secondary batteries. Of these materials, $LiCoO_2$ has been extensively used as a positive electrode material owing to its ease of preparation, high voltage, high specific capacity, and long stable cycle life. $LiCoO_2$ thin film has been deposited using various techniques including radio frequency (RF) magnetron sputtering [3–9], pulsed laser deposition (PLD) [10–12] and the sol–gel method [13–15]. However, as mentioned in many previous reports, the as-deposited $LiCoO_2$ film must be annealed at an elevated temperature of more than 500 °C for crystallization. Such high temperature treatment makes it difficult to utilize flexible polymer film as the substrate because of its low heat resistance.

We previously reported on the preparation of $LiCoO_2$ films using the electron cyclotron resonance (ECR) sputtering method [16]. With this approach we obtained well-crystallized $LiCoO_2$ films without a post-annealing process by adopting favorable deposition conditions. Sputtered $LiCoO_2$ films show good cycle stability and a good discharge property at high current densities. We also reported that $LiCoO_2$ film deposited by the ECR sputtering method with a stoichiometric $LiCoO_2$ target included many impurities, mainly Co_3O_4, and that these impurities were eliminated by adding an excess of Li source to the sputtering target until the atomic ratio of Li/Co was 2.0 [17]. $LiCoO_2$ film sputtered with a Li/Co = 2.0 target exhibited a 1.6 times greater discharge capacity per unit volume than that sputtered with a $LiCoO_2$ target, and provided excellent performance during large current operation.

* Corresponding author. Tel.: +81 46 240 3754; fax: +81 46 270 3721.
E-mail address: takahasi@aecl.ntt.co.jp (M. Takahashi).

0378-7753/$ – see front matter © 2008 Elsevier B.V. All rights reserved.
doi:10.1016/j.jpowsour.2008.09.108

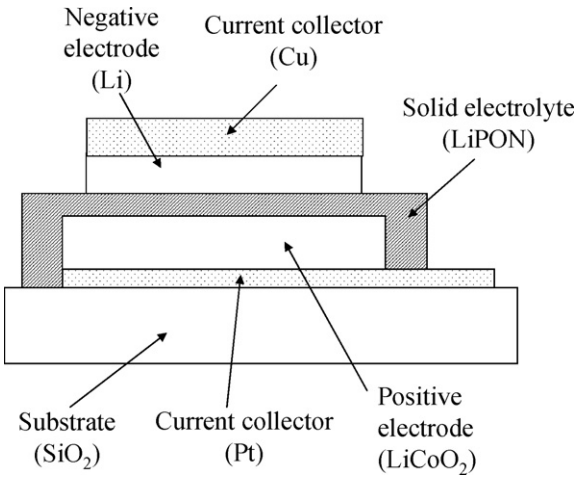

Fig. 1. Schematic illustration of the all-solid-state lithium secondary battery.

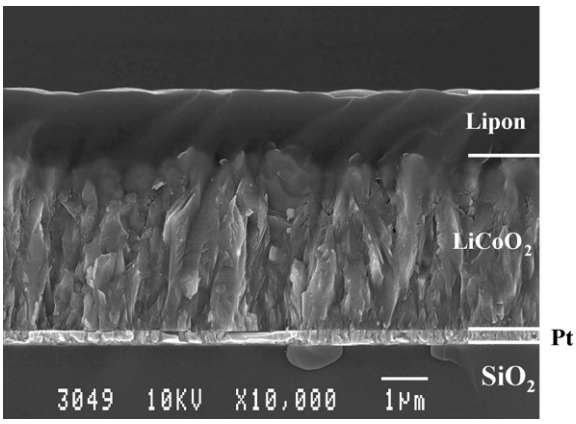

Fig. 2. SEM image of a cross-sectional view of the ECR sputtered $LiCoO_2$ film covered with a LiPON film.

In the present study, we fabricated all-solid-state lithium secondary batteries consisting of $LiCoO_2$ thin films prepared by ECR sputtering LiPON and metallic lithium films, and investigated the influence of the sputtering target composition on the large current discharge and charge–discharge cycle performance of the all-solid-state batteries. We also investigated the crystallographic characterization of the $LiCoO_2$ films deposited by using targets with various compositions before and after a charge–discharge cycle performed in an ordinary liquid electrolyte. We used X-ray diffraction analysis and Raman spectroscopy to characterize the crystallinity of the film, and we considered the reason for the capacity decrease during the charge–discharge cycle test using the experimental results we obtained (Fig. 1).

2. Experimental

A schematic illustration of the all-solid-state lithium secondary battery is shown in Fig. 1. We prepared the $LiCoO_2$ films by ECR sputtering on a Pt current collector formed on a quartz substrate by using AFTEX-EC3400 (MES AFTY Corporation). We formed the sputtering targets by sintering a mixture of $LiCoO_2$ and Li_2CO_3 powder as the Li/Co molar ratios of the targets were 1.0, 1.2, 1.7 and 2.0. Hereafter, we refer to a target where Li/Co = x as a Lix target. The films were sputtered with microwave and RF powers of 800 and 500 W, respectively, in a mixture atmosphere of argon and oxygen ($Ar:O_2$ = 40:1). The total gas pressure was regulated at 0.14 Pa. Substrates were heated at 300 °C during sputtering. The other sputtering conditions have been reported elsewhere [16]. A Pt current collector was prepared by RF magnetron sputtering using an SPF-430H (ANERVA Corporation). The films were sputtered with an RF power of 100 W in an argon atmosphere of 1 Pa. The Pt films were about 500-nm thick. We prepared the all-sold-state batteries by depositing LiPON film on $LiCoO_2$ by RF magnetron sputtering and depositing metallic lithium film on the LiPON film by vacuum evaporation. The LiPON film was deposited by using an SPL-210 (ANERVA Corporation) with an RF power of 100 W in a nitrogen atmosphere of 1 Pa. Li_3PO_4 was used as a sputtering target and the LiPON films were about 1.5 μm thick. Fig. 2 shows a SEM image of a cross-sectional view of the ECR sputtered $LiCoO_2$ film covered with a LiPON film. The $LiCoO_2$ film was sputtered with a Li1.2 target. Both the $LiCoO_2$ and LiPON films are fairly compact and are in contact with each other with no clearance. The $LiCoO_2$ films sputtered with Li1.0 and Li1.7 targets exhibited similar morphology to the film shown in Fig. 2, and the film sputtered with a Li2.0 target had a somewhat small columnar structure. A Li anode and Cu current collector were deposited in a vacuum below 10^{-3} Pa. After sputtering the LiPON film, we handled the samples in dry air at a dew point of less than −50 °C. The crystal structure of the deposited $LiCoO_2$ films was investigated using X-ray diffraction (XRD) analysis with an RINT 2100HF (Rigaku Co. Ltd.) with Cu Kα radiation. The angle of the incident radiation to the substrate plane was fixed at 5° and the detector was moved through an angle of 2-theta. Raman spectroscopy with a Super Labram (Dilor Co.) was also adopted to investigate the crystalline phases in the sputtered $LiCoO_2$ film. We investigated the electrochemical property of the all-solid-state batteries by employing a charge–discharge cycle test. The cycle test was carried out galvanostatically between 3.0 and 4.3 V by using a Mac Pile II system (Bio-logic) in dry air. We also used a three-electrode beaker type cell to investigate the properties of the $LiCoO_2$ film in the liquid electrolyte. The sputtered $LiCoO_2$ film on the quartz substrate with Pt film was used as a working electrode. A lithium metal sheet and a lithium fragment were used as counter and reference electrodes, respectively. 1 mol dm^{-3} of $LiPF_6$ in ethylene carbonate/dimethyl carbonate (1:1, v/v) was used as the electrolyte.

3. Results and discussion

When using the ECR sputtering method to deposit $LiCoO_2$ film, the composition of the sputtering target influenced the characteristics of both the $LiCoO_2$ film and an all-solid-state battery employing the $LiCoO_2$ film. These characteristics include the surface morphology, crystallinity and discharge capacity [17]. In this study, we investigated the effect of the target composition on the discharge curves and the charge–discharge cycle performance of an all-solid-state battery employing $LiCoO_2$ film deposited by ECR sputtering. Fig. 3(a) and (b) shows the influence of the discharge current on the discharge curves of all-solid-state batteries employing $LiCoO_2$ films sputtered with Li2.0 and Li1.0 targets, respectively. The $LiCoO_2$ film sputtered with the Li2.0 target exhibited a 1.6 times greater discharge capacity per unit volume than that sputtered with the Li1.0 target for a 0.1 mA cm^{-2} discharge. We assumed that the small amount of impurity in the film sputtered with the Li2.0 target was the origin this high capacity. We measured the Li/Co ratios of sputtered $LiCoO_2$ films with inductively coupled plasma/atomic emission spectrometry (Seiko Instruments Inc., SPS1700). The Li/Co ratios in the films sputtered with Li1.0, Li1.7 and Li2.0 targets were 0.56, 0.57 and 0.97, respectively. Since the theoretical Li/Co ratio of $LiCoO_2$ is 1.0, the $LiCoO_2$ films sputtered with Li1.0 and Li1.7 targets appear to include some amount of impurity. Since the thickness of the $LiCoO_2$ film prepared with

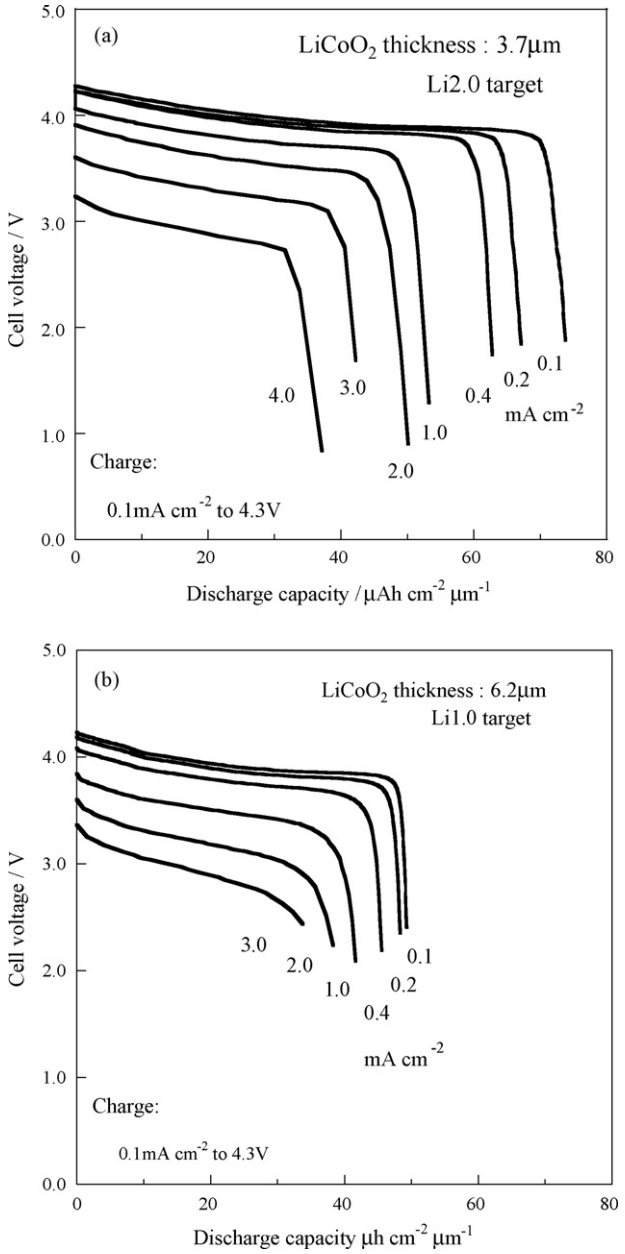

Fig. 3. Influence of discharge current on discharge curves of all-solid-state batteries employing $LiCoO_2$ films. (a) $LiCoO_2$ film was sputtered with a Li2.0 target and (b) $LiCoO_2$ film was sputtered with a Li2.0 target.

the Li2.0 target was adjusted to about 60% of that prepared with the Li1.0 target, both batteries exhibited almost the same discharge capacity per unit area. By comparing the voltage of the plateau region in the discharge curves, we observed that the voltage of the battery employing the $LiCoO_2$ film prepared with the Li2.0 target was higher than that employing the film with the Li1.0 target, especially in curves measured for a high discharge current. For example, with a 3.0 mA cm^{-2} discharge, the voltage of the discharge plateau of the cell employing the $LiCoO_2$ film prepared with the Li2.0 target was higher than 3.0 V. In contrast, that of the cell employing the $LiCoO_2$ film prepared with the Li1.0 target is lower than 3.0 V in the latter half. The ohmic resistance of the $LiCoO_2$ film increases with increasing film thickness. We consider that the voltage drop observed during high current discharge is reduced by reducing the ohmic resistance of the $LiCoO_2$ film, because the

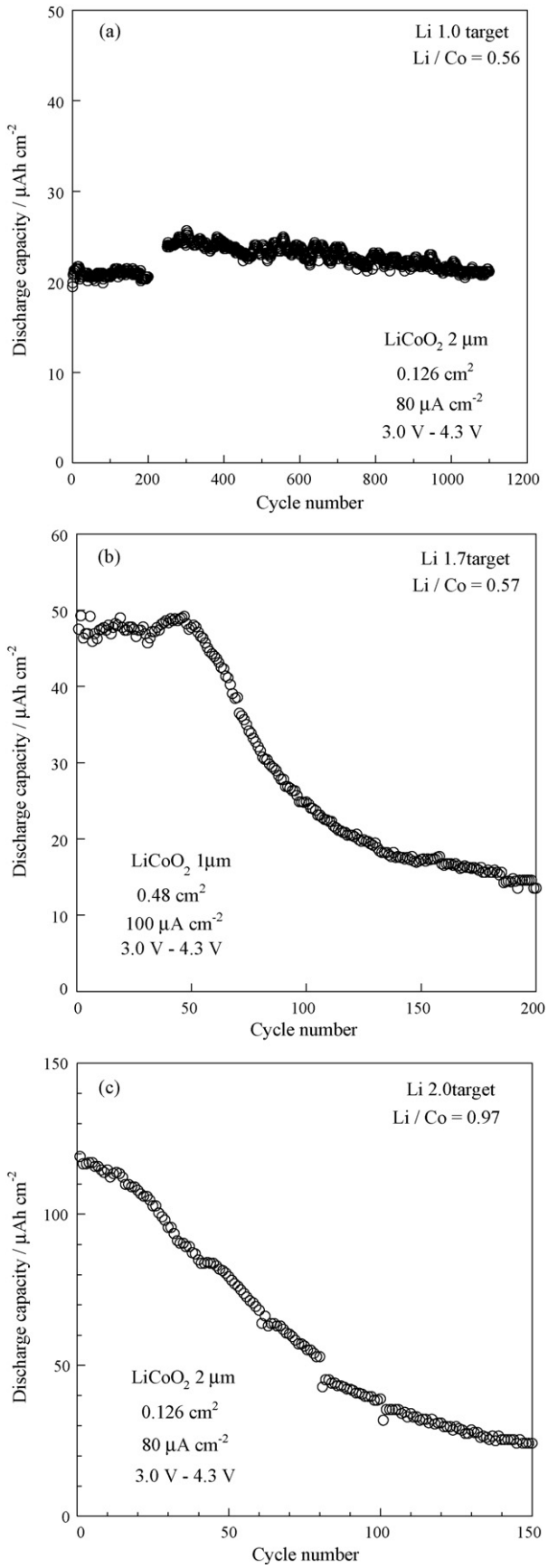

Fig. 4. Cycle performance of all-solid-state batteries employing $LiCoO_2$ film deposited with (a) Li1.0, (b) Li1.7 and (c) Li2.0 targets.

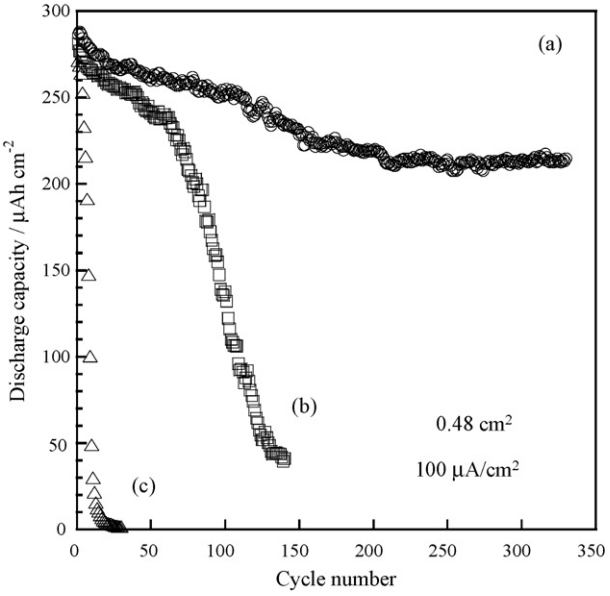

Fig. 5. Cycle performance of $LiCoO_2$ films prepared with (a) Li1.0, (b) Li1.7 and (c) Li2.0 targets measured in the liquid electrolyte.

$LiCoO_2$ film prepared with the Li2.0 target needs less thickness than the film with the Li1.0 target to achieve the same discharge capacity.

Fig. 4 shows the cycle performance of all-solid-state batteries employing $LiCoO_2$ film deposited with (a) Li1.0, (b) Li1.7 and (c) Li2.0 targets. Although, strictly speaking, we cannot compare these batteries in terms of performance since there are certain differences as regards battery size and measurement conditions, we can observe the tendency of the cycle performance of each battery. The cell employing film prepared with the Li1.0 target provided long and stable cycle performance. The cell employing film prepared with the Li1.7 target performed stably for the first 50 cycles, and then the capacity decreased rapidly with cycling. The capacity of the cell employing film prepared with the Li2.0 target decreased continuously during the entire cycle test even though the capacity per unit volume of the $LiCoO_2$ film in the initial cycle was larger than that of the other batteries.

To investigate the mechanism of the capacity decrease in the cycle test, it is important to analyze the structural and compositional changes of the $LiCoO_2$ film. Since the $LiCoO_2$ film is covered with LiPON, Li and Cu film in the all-solid-state battery, it is difficult to analyze the $LiCoO_2$ film after the cycle test. Hence we adopted beaker type cells and measured the cycle performance of $LiCoO_2$ film in liquid electrolyte. Here, we can obtain the bare surface of $LiCoO_2$ film used in the cycle test simply by rinsing off the electrolyte.

Fig. 5 shows the cycle performance of $LiCoO_2$ films prepared by using sputtering targets of various compositions in liquid electrolyte. The film prepared with the Li2.0 target exhibited poor cycle stability. The film prepared with the Li1.7 target performed stably during the first 50 cycles, and then the capacity decreased rapidly with cycling. The film prepared with the Li1.0 target provided long and stable cycle performance. We noted that the dependence of the composition of the target used in $LiCoO_2$ sputtering on the $LiCoO_2$ film cycle performance is similar to that of the all-solid-state battery employing $LiCoO_2$ film as shown in Figs. 4 and 5. If different reactions cause the capacity reduction of the all-solid-state batteries and that of the beaker type cell during the cycle test, for example by the reaction of $LiCoO_2$ and each electrolyte, the

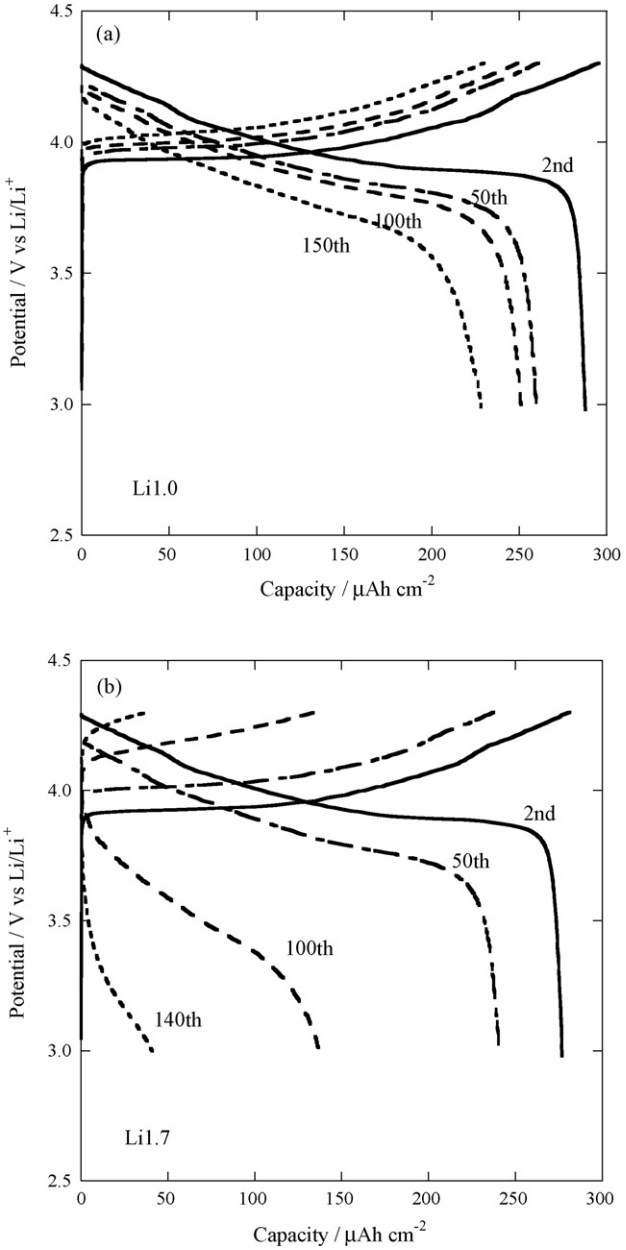

Fig. 6. Transition in charge and discharge curves of (a) $LiCoO_2$ film sputtered with a Li1.0 target and (b) film sputtered with a Li1.7 target in a beaker type cell.

capacity decrease and its target composition dependence should be different in each case. The fact that the all-solid-state cell and the beaker type cell exhibit a similar capacity reduction suggests that this reduction is caused by the deterioration of the $LiCoO_2$ film during the charge–discharge cycle. Fig. 6 shows the change in the charge and discharge curves of (a) the $LiCoO_2$ film sputtered with the Li1.0 target and (b) the film sputtered with the Li1.7 target during a cycle test measured in a beaker type cell. A comparison of the two figures reveals that there is little difference between the curves of the 2nd and 50th cycles. When the Li1.0 target was used, the voltage shift of the curves observed after the 50th cycle was relatively small. In contrast, a voltage shift, especially a voltage drop in the discharge curves, was clearly observed after the 50th cycle when using the Li1.7 target. The capacity decrease of the $LiCoO_2$ film sputtered with the Li1.7 target is caused by this increase in overvoltage in the charge–discharge reaction.

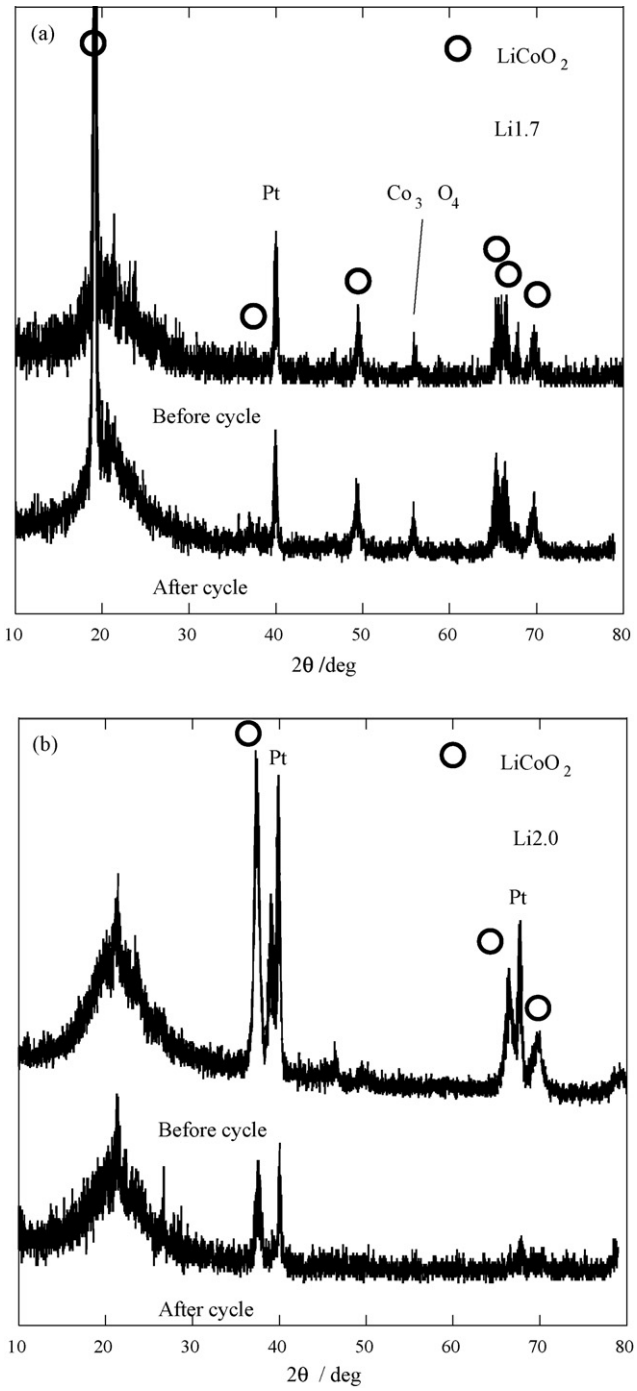

Fig. 7. XRD pattern of the $LiCoO_2$ films measured before and after the cycle test. The measured film sputtered with (a) Li1.7 and (b) Li2.0 targets.

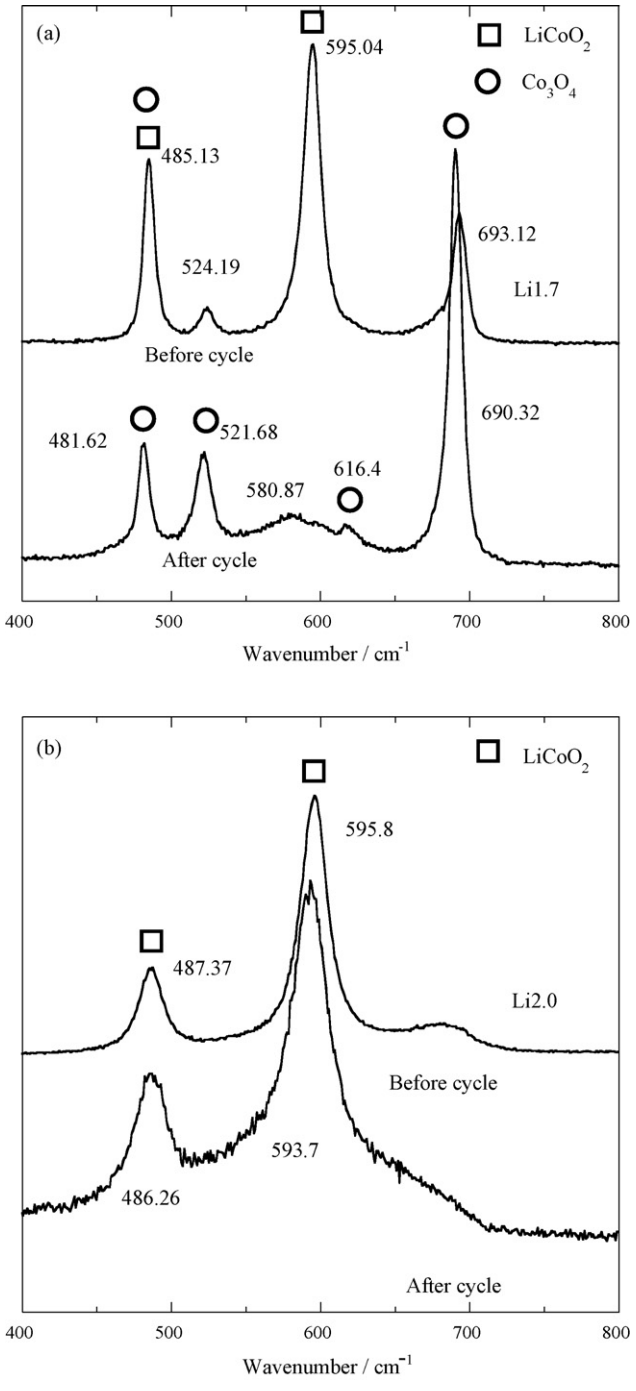

Fig. 8. Raman spectra of the $LiCoO_2$ films measured before and after the cycle test. The measured film sputtered with (a) Li1.7 and (b) Li2.0 targets.

We consider that the reduction in crystallinity and the generation of impurities in the $LiCoO_2$ film are the reasons for the increased overvoltage. To investigate the change in the crystal structure of $LiCoO_2$ film during the cycle test, we measured the XRD pattern and Raman spectrum of the film before and after the cycle test. Several previous studies have reported that there is a correspondence between each peak observed in the Raman spectra and the material, and that Raman spectroscopy is effective for distinguishing the presence of $LiCoO_2$ and Co_3O_4 [18,19]. We could not measure the XRD pattern or Raman spectra of the film sputtered with the Li1.0 target because the cycle test of the film in the liquid electrolyte was terminated by the film peeling from the substrate. Fig. 7(a) shows the XRD pattern of $LiCoO_2$ films sputtered with the Li1.7 target, and (b) shows that of the film sputtered with the Li2.0 target measured before and after the cycle test. With the Li1.7 target, a sharp (0 0 3) peak was observed at around $2\theta = 19^\circ$ and there was little difference between the XRD patterns measured before and after the cycle test. This result indicates that film obtained with the Li1.7 target has good crystallinity that does not change during the cycle test. With the Li2.0 target, the intensity of the $LiCoO_2$ peaks was very weak and decreased after the cycle test. We believe that the crystal structure of the $LiCoO_2$ film prepared

with the Li2.0 target deteriorates as a result of the charge–discharge cycle.

Fig. 8 shows the Raman spectra of $LiCoO_2$ films sputtered with (a) a Li1.7 target and (b) a Li2.0 target measured before and after the cycle test, respectively. We can observe peaks corresponding to HT–$LiCoO_2$ (about 485 and 594 cm^{-1}) and peaks corresponding to Co_3O_4 (about 522 and 693 cm^{-1}) in the Raman spectrum measured before the cycle test as shown in Fig. 7(a). In contrast, the peaks corresponding to HT–$LiCoO_2$ had almost disappeared from the Raman spectrum measured after the cycle test and only the peaks corresponding to Co_3O_4 were observed as shown in Fig. 7(b). This disappearance of $LiCoO_2$ contradicts the XRD analysis result. As shown in Fig. 7(a), the XRD measurement confirmed that both $LiCoO_2$ and Co_3O_4 were present in the film used in the cycle test. We assumed that the crystal structure of the $LiCoO_2$, which is the active material in the charge–discharge cycle, that was present in the surface region of the $LiCoO_2$ film deteriorated during the cycle test, and an inactive layer of Co_3O_4 was formed on the surface of the $LiCoO_2$ film. Since it was reported previously that disproportionation of the $LiCoO_2$ power in a non-aqueous electrolyte generated Co_3O_4 [20], $LiCoO_2$ in the surface region may change to Co_3O_4. Raman spectroscopy is more sensitive to surface material than XRD analysis, and so it clearly indicated the presence of a Co_3O_4 surface layer. This Co_3O_4 surface layer inhibits the Li diffusion or charge transfer reaction and causes an increase in overvoltage and a capacity reduction.

With the Li2.0 target, only the $LiCoO_2$ peaks were observed in the spectra obtained before and after the cycle test. However, we can see that the peak intensity measured after the cycle test was smaller than that measured before the cycle test by comparing the noise levels of the two spectra shown in Fig. 8(b). This result is consistent with the change in the XRD pattern seen in Fig. 7(b). This deterioration of the crystal structure seems to reduce the capacity. We consider that the presence of Co_3O_4 affects the crystal structure of the sputtered films and structural deterioration because the properties of the $LiCoO_2$ film sputtered with the Li2.0 target such as surface morphology, crystal structure and electrochemical performance, were very different from those of films sputtered with Li1.7 and Li1.0 targets [17]. The reduction in the capacity during the cycle test measured in the beaker type cell was much faster than that in the all-solid-state battery. The $LiCoO_2$ films in the all-solid-state batteries were securely covered with solid electrolyte film and this covering is assumed to suppress the deterioration of crystal structure compared with the film in the beaker type cell.

4. Conclusion

We investigated the influence of the sputtering target composition on the performance of all-solid-state batteries employing $LiCoO_2$ film deposited by the ECR sputtering method. The capacity of a battery employing $LiCoO_2$ film sputtered with a Li2.0 target decreased more rapidly than that sputtered with a Li1.0 or Li1.7 target during a charge–discharge cycle test. We also investigated the cycle performance of $LiCoO_2$ films in ordinary liquid electrolyte by using beaker type cells. We found that the reduction in capacity during the cycle tests was caused by the deterioration of the $LiCoO_2$ film, because the dependence of the target composition on the cycle performance in the beaker type cells was similar to that in the all-solid-state cells. We consider that the capacity reduction was caused by the deterioration of the crystallinity of the $LiCoO_2$ film when using the Li2.0 target and by the formation of a Co_3O_4 layer on the surface of the $LiCoO_2$ film as a result of the deterioration of the crystal structure of $LiCoO_2$ of the surface region when using the Li1.7 target from the results of X-ray diffraction and Raman spectra analyses. We believe that the existence of Co_3O_4 affects the crystal structure of the sputtered films and the deterioration of the structure in a cycle test.

Acknowledgements

The authors are indebted to Tadahito Aoki of NTT Energy and Environment Systems Laboratories for helpful guidance and discussions. The authors also thank Mr. Hiroshi Ando of NTT Advanced Technology Corporation for undertaking the Raman spectroscopy measurements.

References

[1] J. Yamaki, H. Ohtsuka, T. Shodai, Solid State Ionics 86–88 (1996) 1279.
[2] H. Ohtsuka, Y. Sakurai, Solid State Ionics 144 (2001) 59.
[3] J.B. Bates, N.J. Dudney, B.J. Neudecker, F.X. Hart, H.P. Jun, S.A. Hackney, J. Electrochem. Soc. 147 (2000) 59.
[4] J.B. Bates, N.J. Dudney, B. Neudecker, A. Ueda, C.D. Evans, Solid State Ionics 135 (2000) 33.
[5] Y. Jang, N.J. Dudney, D.A. Blom, L.F. Allard, J. Power Sources 119 (2003) 195.
[6] N.J. Dudney, Y. Jang, J. Power Sources 119–121 (2003) 300.
[7] J.F. Whitacre, W.C. West, E. Brandon, B.V. Ratnakumar, J. Electrochem. Soc. 148 (2001) A1078.
[8] H. Kim, Y.S. Yoon, J. Vac. Technol. A 22 (2004) 1182.
[9] C.-L. Liao, K.-Z. Fung, J. Power Sources 128 (2004) 263.
[10] H. Xia, L. Lu, G. Ceder, J. Power Sources 159 (2006) 1422.
[11] Y. Iriyama, M. Inaba, T. Abe, Z. Ogumi, J. Power Sources 94 (2001) 175.
[12] Y. Iriyama, H. Kurita, I. Yamada, T. Abe, Z. Ogumi, J. Power Sources 137 (2004) 111.
[13] M. Kim, K. Park, D. Kim, J. Son, H. Kim, J. Kor. Ceram. Soc. 38 (2001) 777.
[14] S.G. Kang, S.Y. Kang, K.S. Ryu, S.H. Chang, Solid State Ionics 120 (1999) 155.
[15] Y.H. Rho, K. Kanamura, T. Umegaki, J. Electrochem. Soc. 150 (2003) A107.
[16] M. Hayashi, M. Takahashi, Y. Sakurai, J. Power Sources 174 (2007) 990.
[17] M. Hayashi, M. Takahashi, T. Shodai, Abstract of the 14th International Meeting on Lithium Batteries, Abstract #345 (2008).
[18] L. Mendoza, R. Baddour-Hadjean, M. Cassir, J.P. Pereira-Ramos, Appl. Surf. Sci. 225 (2004) 356.
[19] K.-S. Han, S.W. Song, M. Yoshimura, J. Am. Ceram. Soc. 81 (1998) 2465.
[20] D. Aurbach, B. Markovsky, G. Salitra, E. Markevich, Y. Talyossef, M. Koltypin, L. Nazar, B. Ellis, D. Kovacheva, J. Power Sources 165 (2007) 491.